Int. J. Morphol.,
44(2):599-609, 2026.

Antineoplastic and Immunomodulatory Effects of *Falcaria vulgaris* L. in Cervical Cancer: Insights in C57BL/6 Mouse Papilloma Model

Efectos Antineoplásicos e Inmunomoduladores de *Falcaria vulgaris* L. en Cáncer de Cuello Uterino: Perspectivas en el Modelo de Papiloma Murino C57BL/6

Cuiyun Lu[1]; Shujun Yan[2]; Mengjuan Chen[1]; Zhen Zhao[1]; Lihua Li[1] & Bin Lu[1]

LU, C.; YAN, S.; CHEN, M.; ZHAO, Z.; LI, L. & LU, B. Antineoplastic and immunomodulatory effects of *Falcaria vulgaris* L. in cervical cancer: Insights in C57BL/6 mouse papilloma model. *Int. J. Morphol., 44(2)*:599-609, 2026.

SUMMARY: This study aimed to assess the anticancer and immunomodulatory effects of the aqueous extract of *Falcaria vulgaris* L. (FV) on cervical cancer *in vivo* model. For the tumor retardation study, a C57BL/6 mouse papilloma (Pa) model was employed. The mice were divided into six groups: normal control (NC), papilloma control (PaC), PaC treated with cisplatin (PaC + Cis) at a dosage of 4 mg/kg body weight, PaC treated with FV at doses of 150 and 300 mg/kg body weight (PaC + 150 and 300 FV), and PaC treated with FV at doses of 300 mg/kg body weight and Cisplatin (PaC + 300 FV + Cis). The mice received daily oral gavage of FV for 14 days, while Cisplatin (Cis) was administered intravenously on the 1st, 5th, and 9th days. Hematological and biochemical parameters were evaluated using a hematology analyzer and various kits. The expression of E6, E7, p53, and Caspase-3 genes in tumor samples was quantified using qPCR, and Th1, IL-6, IL-1β, and Th2 cytokine levels were measured via ELISA. FV caused upregulated tumor suppressor proteins (p53 and Caspase-3) while downregulating viral oncoproteins (E6 and E7). In the mouse papilloma model, FVE significantly reduced tumor volume and weight and induced immunomodulatory effects in the animals. Specifically, it elevated serum levels of IL-2 (Th1) and decreased levels of IL-10 (Th2), IL-6, and IL-1β cytokines. Notably, FV did not adversely affect the body weight, food intake, or organ histopathology of the mice. FV demonstrated significant anticancer and immunomodulatory effects against cervical cancer cells and in a female mouse papilloma model.

KEY WORDS: *Falcaria vulgaris* L.; Cervical cancer; Apoptosis; Mouse papilloma model.

INTRODUCTION

Cervical cancer ranks as the second most common cause of cancer-related mortality among women in India and fourth globally. Conventional treatment protocols involving surgical intervention, chemotherapy, and radiotherapy often lead to significant adverse effects, compounded by challenges of therapeutic resistance and disease recurrence. This has prompted growing interest in complementary and alternative medicine (CAM) approaches as supplementary therapies (Cohen *et al*., 2019). Botanical-based treatments, a primary component of CAM modalities, demonstrate dual anticancer and immune-regulating capabilities. Contemporary clinical observations suggest these natural adjuncts may mitigate treatment-related complications while potentially enhancing long-term remission outcomes in oncology patients (Lagu *et al*., 2024). Recent investigations into botanical interventions for papillomavirus management have identified several promising candidates.

Curcumin, primarily through its curcuminoid constituents, demonstrates multimodal activity by inhibiting HPV oncoproteins E6/E7, reducing viral genomic integration in vitro, and enhancing radiosensitivity in murine models, with Phase II trials currently evaluating its efficacy against cervical intraepithelial neoplasia (Zhao *et al*., 2024). Green tea polyphenols, particularly epigallocatechin-3-gallate (EGCG), exhibit both preventive and therapeutic potential through L1 protein-mediated viral entry blockade and HPV16 oncogene suppression, evidenced by 80 % wart regression in canine models and successful human trials for genital wart clearance. Fungal derivatives like AHCC from medicinal mushrooms enhance NK cell cytotoxicity, achieving 60 % HPV eradication in clinical cohorts while synergizing with interferon therapies in experimental models (Yap *et al*., 2021). Papaya leaf extracts containing carpaine and flavonoids demonstrate 45 % viral load reduction in

[1] Obstetrics and Gynecology, Zhoukou Maternal and Child Health, Hospital (Zhoukou Children's Hospital), Zhoukou City, Henan Province, China.
[2] Pregnancy Health Care Department, Zhoukou Maternal and Child, Health Hospital (Zhoukou Children's Hospital), Zhoukou, City, Henan Province, China.
Funding: This research has received support. Project Number: 252102310200. Project Name: Henan Provincial Science and Technology Department, 2025 Henan Provincial Science and Technology Innovation Project.

Received: 2025-10-01 Accepted: 2025-11-05

lagomorph studies through dual antiviral and Th1 immunomodulatory mechanisms, complemented by anti-angiogenic properties in neoplastic lesions (Haber *et al*., 2023). Neem constituents azadirachtin and nimbolide induce complete cutaneous wart resolution in clinical observations within 21 days, mechanistically interfering with viral capsid assembly and preventing malignant transformation in hamsterbuccal models (Raman & Elengoe, 2021). The Brazilian pepper tree's NF-κB inhibitory activity underlies its dose-dependent virucidal effects, showing 70 % lesion size reduction in equine studies. Emerging phytocompounds including mistletoe lectins, gingerol, and sulforaphane from broccoli sprouts present novel mechanisms targeting viral episome maintenance and transformed cell apoptosis (Salaria *et al*., 2022). While these botanical agents show therapeutic promise, challenges persist in extract standardization and bioavailability optimization, with most clinical evidence remaining preliminary (Phase I/II). Contemporary research emphasizes combination strategies integrating plant extracts with conventional modalities like cryotherapy, demonstrating superior clearance rates compared to monotherapies. Patients considering these adjunctive approaches should prioritize consultation with oncology specialists to ensure therapeutic compatibility and safety (Chen *et al*., 2019).

Falcaria vulgaris L. (FV- Apiaceae family), commonly known as sickleweed, is a perennial herb characterized by serrated linear leaves and white umbellate inflorescences, native to Eurasia but invasive in disturbed habitats globally. Phytochemical analyses reveal a rich profile of bioactive compounds, including monoterpene-dominated essential oils (a-pinene, limonene), immunomodulatory flavonoids (quercetin, kaempferol), and polyacetylenes such as falcarinol—a compound unique to Apiaceae with demonstrated membrane-disruptive properties (Zangeneh *et al*., 2019). Traditionally employed for wound healing and gastrointestinal disorders, modern studies validate its hepatoprotective, antioxidant, and antidiabetic activities, linked to phenolic acids like chlorogenic acid. Antimicrobial evaluations show broad-spectrum efficacy, with essential oil extracts inhibiting *Staphylococcus aureus* (MIC: 64 mg/mL) and *Pseudomonas aeruginosa*, while coumarins and polyacetylenes suggest indirect antiviral potential through protease inhibition and virucidal mechanisms observed in related species (Kohsari *et al*., 2019). Immunomodulatory effects include NF-κB pathway suppression, reduced pro-inflammatory cytokines (TNF-α, IL-6), and enhanced NK cell activity, positioning it as a candidate for viral immune regulation. Although direct evidence against papillomavirus remains unexplored, its falcarinol-mediated interference with viral entry mechanisms (via L1 protein interaction) and Th1/Th17 balance modulation propose theoretical efficacy against HPV persistence (Zoric *et al*., 2022). Current gaps highlight the need for targeted studies on HPV oncoprotein inhibition and clinical translation of its bioactive synergies, particularly in combination with conventional antiviral therapies. This study aims to investigate the dual antineoplastic-immunomodulatory mechanisms of FV in cervical cancer through integrated analysis of *in vivo* C57BL/6 mouse papilloma model, with emphasis on HPV-associated oncogenic pathway modulation and tumor microenvironment reprogramming.

MATERIAL AND METHOD

Preparation of FV

Fresh *Falcaria vulgaris* (FV) biomass (9 kg) underwent low-temperature dehydration at 34 °C under light-restricted conditions to prevent photochemical degradation, with botanical authentication by a certified taxonomist. The desiccated material was mechanically pulverized into a homogeneous fine powder (particle size <500 μm) using a stainless-steel grinder. The powdered biomass underwent binary solvent extraction in a 50:50 (v/v) ethanol-acetone mixture at 35 °C for 72 h under continuous orbital agitation (150 rpm). The crude extract was sequentially filtered through Whatman No. 1 filter paper, followed by vacuum-assisted clarification. The filtrate was concentrated to a semisolid consistency using a Buchi R-300 rotary evaporator (40 °C, 150 mbar), yielding 320 g of FV-based ointment, which was aliquoted into amber vials for storage at 4 °C. Prior to therapeutic application, a preclinical safety assessment was conducted via epicutaneous patch testing on five female C57BL/6 mice (8–10 weeks old), with continuous monitoring for erythema, edema, and pruritic responses during a 48-hour observation period under controlled laboratory conditions (Basatinya *et al*., 2021).

Experimental design (animals and maintenance, acute toxicity study)

Female Swiss albino mice (6-8 weeks old) and C57BL/6 mice (6-8 weeks old) were sourced from Xuzhou Mining group general hospital for acute toxicity and tumor retardation studies respectively, with all specimens maintained under OECD-compliant conditions featuring 25±4 °C ambient temperature, 40±3 % relative humidity, and 12-hour photoperiod cycles in polypropylene cages, including a 72-hour acclimatization period with *ad libitum* access to standardized feed and water. For the OECD 423-guided acute toxicity assessment, Swiss albino mice (18-22 g) were stratified into two groups (n=3/group): Group I received distilled water (vehicle control) while Group II received 2000 mg/kg bw PVaq via oral gavage, followed by intensive clinical monitoring during acute (0-4 h) and

subacute (14-day) phases for behavioral alterations, physiological distress, and mortality. Terminal necropsy included macroscopic evaluation of cardiopulmonary (heart, lungs), hepatobiliary (liver), renal (kidneys), and reproductive (uterus, ovaries) systems for pathological manifestations, with pre-terminal body weight recordings and post-mortem organ inspections conducted to identify toxicity indicators (Aphale *et al*., 2021).

Tumor induction and animal grouping

Tumorigenesis was initiated in C57BL/6 mice through subcutaneous implantation of TC-1 cells (1×10^6 cells/mouse) in the right flank, following established oncological models (Deshpande *et al*., 2019). Five days post-inoculation when tumors became palpable (≥2 mm^3), subjects were stratified into six experimental cohorts (n=10/group): Normal Control (NC), Papilloma Control (PaC), PaC+Cisplatin (PaC+Cis) (4 mg/kg bw IV), PaC+150 FV (150 mg/kg bw oral), PaC+300 FV (300 mg/kg bw oral), and PaC+300 FV+Cis combination therapy. The FV extract was administered daily via oral gavage over 14 days, while cisplatin injections were delivered intravenously on days 1, 5, and 9 using an optimized intermittent dosing schedule.

Tumor progression was monitored through bi-dimensional measurements using digital calipers, with volumes calculated via the modified ellipsoid formula:

$$V=1/2\times W^2\times L$$

where V = tumor volume (mm^3), L = longitudinal diameter, and W = transverse diameter (Fig. 1) (Aphale *et al*., 2021; Huang *et al*., 2021).

Hematological and biochemical

During the terminal phase of the tumor retardation study, subjects underwent overnight fasting prior to comprehensive biological sampling. Hematological profiling was conducted via retro-orbital blood collection followed by necropsy, utilizing a Mindray-BC2800Vet analyzer to quantify complete blood parameters: granulocyte-macrophage colony-stimulating factor (GM-CSF), granulocyte colony-stimulating factor (G-CSF), PLT (platelets), WBC (white blood cell), and RBC (red blood cell). Serum concentrations of IL-2 and IL-10 were quantified using a commercial mouse Th1/Th2 ELISA kit (assay sensitivities: 4 pg/mL for IL-2, 2 pg/mL for IL-10) (Larsson *et al*., 2019).

Histopathological analysis

Systemic organ harvesting encompassed kidneys, tumor, lungs, and ovaries tissues. Tissue specimens underwent standardized paraffin embedding protocols, with 5 mm-thick sections microtomed from tissue blocks and

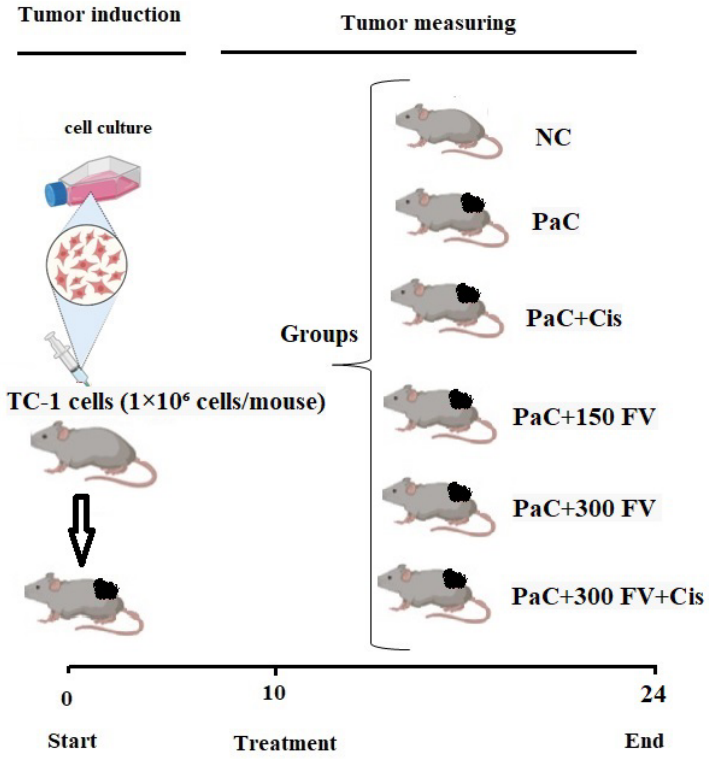

Fig. 1. Research time line and animal grouping.

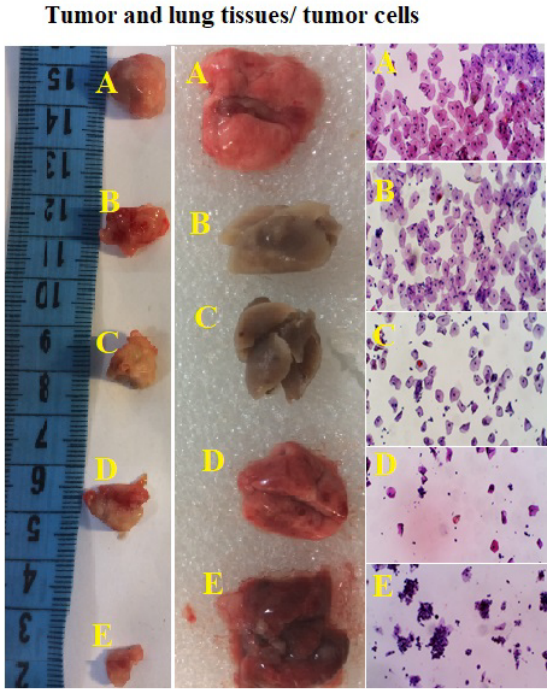

routinely stained with hematoxylin-eosin (H&E) for structural visualization. Systematic histomorphometric analysis of tissues architecture was conducted using an Olympus BX61TRF motorized light microscope equipped with advanced brightfield optics, focusing on key anatomical compartments. High-resolution digital imaging coupled with ImageJ software enabled quantitative assessment of histological parameters, maintaining rigorous protocol standardization across all tissue samples.

Tissue sections were digitized using a high-resolution slide scanner (40x magnification, 0.25 μm/pixel resolution) and preprocessed via stain normalization (Reinhard's method) to standardize hematoxylin/eosin staining intensities. Tumor regions were segmented using threshold-based algorithms (Otsu's method) in QuPath, with manual refinement to exclude stromal or necrotic areas. Heatmaps were constructed in Python using matplotlib and seaborn, with pixel intensities normalized (0–100 % scale) and visualized via the viridis colormap to highlight intratumoral heterogeneity. Linear interpolation smoothed spatial transitions, and heatmaps were overlaid onto original slides for anatomical correlation. Validation included Moran's I spatial autocorrelation analysis ($p<0.01$) and dual-pathologist review ($\kappa = 0.85$) to confirm alignment with histopathological features (Pocock *et al*., 2022).

Tumor tissue E6, E7, p53, and Caspase-3 gene expression

Total RNA was isolated from tumor tissues using TRIzol Reagent (Invitrogen) followed by RNeasy Mini Kit (Qiagen) purification according to manufacturer protocols (Ambion, China), with 5 mg of RNA used for cDNA synthesis. HPV 16 E6/E7 mRNA expression was analyzed via Applied Biosystems StepOne Real-Time PCR using specific primers (p53: F-CACAAAAACAGGTTAAACCCAG/R-AGCACATAGGAGGCATCAG; caspase3: F-ATGGAAGCGAATCAATGGACT/R-CTGTACCAGACCGAGATGTCA; E6: F-ACAAACCGTTGTGTGATTTGTT/R-CAGTGGCTTTTGACAGTTAATACA; E7: F-GAACCGGACAGAGCCCATTA/R-ACACTTGCAACAAAAGGTTACA; GAPDH: F-ACACAGCCGCATCTTCTT/R-CTTGCCGTGGGTAGAGTC). Reactions contained 2X Power SYBR™ Green Master Mix (Thermo Fisher #4367659), 1mL each primer (10 μM), 10-20 ng/μL cDNA, and nuclease-free water to 20 μL final volume, with template-free negative controls. Thermal cycling comprised: 50 °C/2 min, 95 °C/10min, then 40 cycles of 95 °C/30 s and 60 °C/30 s. Gene expression was normalized to GAPDH using the DDCt method and fold change, with triplicate duplicate runs yielding averaged values for quantification.

The fold formula change = $2^{-\Delta\Delta CT}$; $\Delta\Delta Ct = [(Ct_{sample} - Ct_{GAPDH\ gene}) - (Ct_{sample} - Ct_{control})]$.

with Image J software (Zhou *et al*., 2023).

Immunohistochemistry (IHC) assay

The expression levels of p53 proteins in tumor tissues are examined as indicators of apoptotic differentiation. The procedure begins with the washing of tumor tissues using PBS, followed by routine tissue processing. Paraffin blocks are then created using the ovaries, and 5 μm slices of tissue are placed onto slides. Next, all slides are subjected to incubation at 95 °C overnight, followed by another incubation at 25 °C for 1 hour with primary antibodies for p53 tumor tissues. Tween-20 is utilized as a washing buffer, while bovine serum albumin (5 %) is used to block any residual antibodies. Subsequently, the slides are exposed to 3 % hydrogen peroxide (H_2O_2) at 25 °C for 20 min, followed by 3,3'-diaminobenzidine (DAB) staining. Hematoxylin is applied as a counterstain to all slides. The evaluation of the slides is performed using an optical microscope connected to ImageJ software at a magnification of 100X. The percentage (%) of p53 positive cells relative to all cells is determined by analyzing 10 random fields of view in each sample (Vial *et al*., 2025).

Statistical analysis

All experiments employed triplicate biological replicates, with quantitative data expressed as mean ± standard deviation (SD) and analyzed through one-way ANOVA. Results were subjected to two-way ANOVA (significance threshold $p<0.05$). Statistical computations were executed using GraphPad Prism version 7.0 (GraphPad Software, San Diego, CA), maintaining rigorous validation through three independent experimental iterations for *in vivo* paradigms.

RESULTS

Effects of FV on body weight (BW), tumor volume (TV) as well as Kaplan-Meier survival curve

Analysis of body weight (BW), tumor volume (TV), and survival rate measurements across treatment groups revealed that the PaC group showed significant reductions in BW and survival rate ($p<0.05$) along with increased TV compared to the NC group. The addition of Cis to PaC further reduced BW but only moderately decreased TV ($p>0.05$). Notably, FV co-administration at both 150 mg and 300 mg doses significantly improved BW and survival rate ($p<0.05$) compared to PaC alone, with the 300 mg FV

group demonstrating near-normalization of BW. The most pronounced TV reduction occurred in the PaC + 300 FV + Cis group ($p<0.05$), which exhibited synergistic efficacy in tumor suppression while maintaining better weight preservation than Cis-containing regimens without FV (Fig. 2a,b).

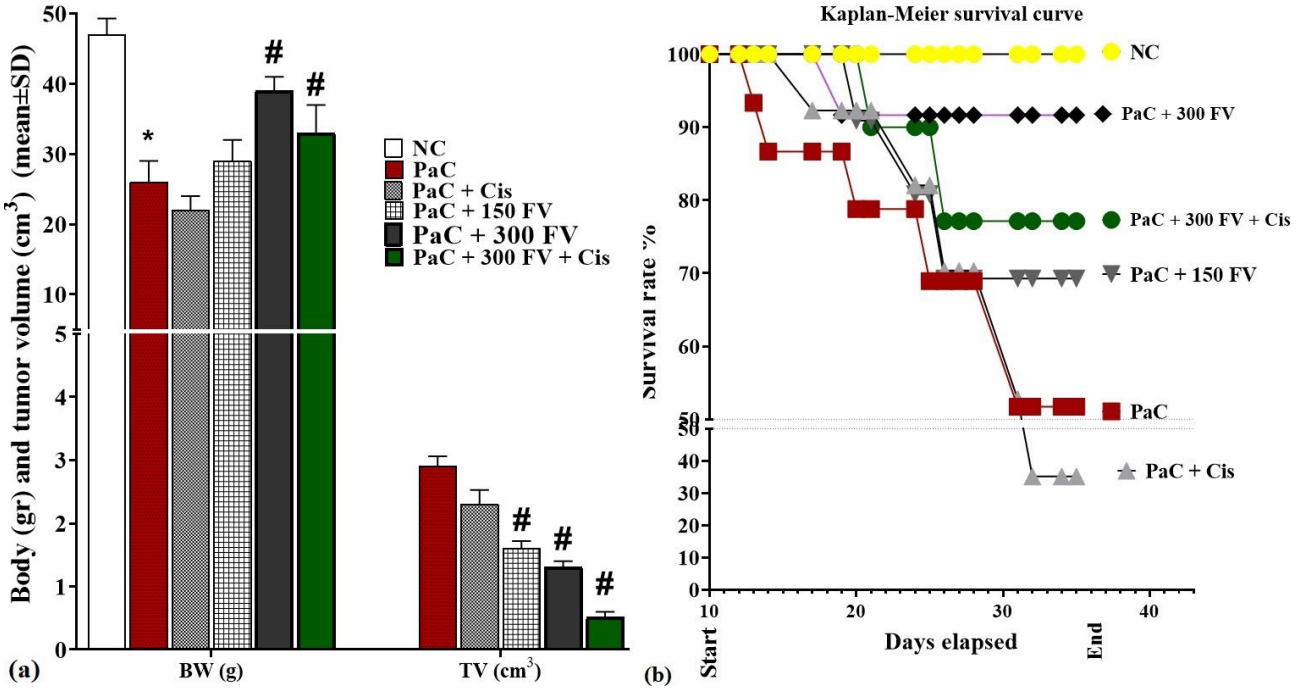

Fig. 2. a. Body weight (BW) (g) and tumor volume (TV) (cm^3) and b. Kaplan-Meier survival curve in different groups (mean±SD). *Significant ($p< 0.05$) difference between papilloma control group (PaC) *versus* the normal control group (NC), #Significant ($p<0.05$) difference between all treatment groups *versus* the papilloma control group (PaC).

Effects of FV on blood cells count, as well as GM-CSF, G-CSF, IL-6, IL-1β, Th1, Th2, and PF4 levels

Analysis of platelet count (PLTs), white blood cells (WBCs), and red blood cells (RBCs) across treatment groups revealed that PaC administration caused significant hematological depletion compared to NC controls ($p<0.05$). Cis supplementation exacerbated PLTs and WBCs reduction while showing limited impact on RBCs ($p>0.05$). FV co-treatment at both 150 mg and 300 mg doses demonstrated dose-dependent hematological recovery ($p<0.05$), with the 300 mg FV group achieving near-normalization of PLTs and WBCs. The FV and Cis combination (PaC + 300 FV + Cis) exhibited the most balanced hematological profile, maintaining superior PLT and RBC preservation compared to Cis-containing regimens without FV ($p<0.05$), while showing synergistic hematoprotective effects against chemotherapy-induced cytopenia (Fig. 3a).

Analysis of platelet factor-4 (PF-4), granulocyte colony-stimulating factor (G-CSF), and granulocyte-macrophage colony-stimulating factor (GM-CSF) levels across treatment regimens revealed distinct cytokine modulation patterns. PaC administration induced marked PF-4 elevation alongside substantial G-CSF and GM-CSF depletion compared to NC controls. Cis supplementation paradoxically attenuated PaC-induced PF-4 increases while further suppressing G-CSF levels. FV co-administration demonstrated dose-dependent cytokine restoration, with 300 mg FV achieving near-baseline GM-CSF levels and partial G-CSF recovery. The FV and Cis combination (PaC + 300 FV + Cis) exhibited synergistic modulation, normalizing PF-4 to below control levels while maintaining intermediate G-CSF values that surpassed Cis-only regimens, suggesting balanced immunoregulatory effects between hematoprotection and chemotherapy efficacy (Fig. 3b).

Analysis of Th1 and Th2 as well as proinflammatory cytokines (IL-1β, IL-6) revealed significant immunomodulatory effects across treatment regimens. In PaC group induced marked Th2 polarization ($p<0.05$) accompanied by substantial IL-1β and IL-6 elevation compared to NC controls. Cis supplementation further amplified Th2 dominance while only marginally affecting cytokine levels ($p>0.05$). FV demonstrated dose-dependent attenuation of PaC-induced immune dysregulation, with 300

mg FV achieving near-normalization of Th1/Th2 balance and significant cytokine reduction ($p<0.05$). The FV and Cis (PaC + 300 FV + Cis) exhibited synergistic immunomodulation, maintaining intermediate Th1 levels and cytokine concentrations that significantly outperformed Cis-containing regimens without FV ($p<0.05$), suggesting preserved antitumor immunity while mitigating chemotherapy-associated inflammatory responses (Fig. 3c).

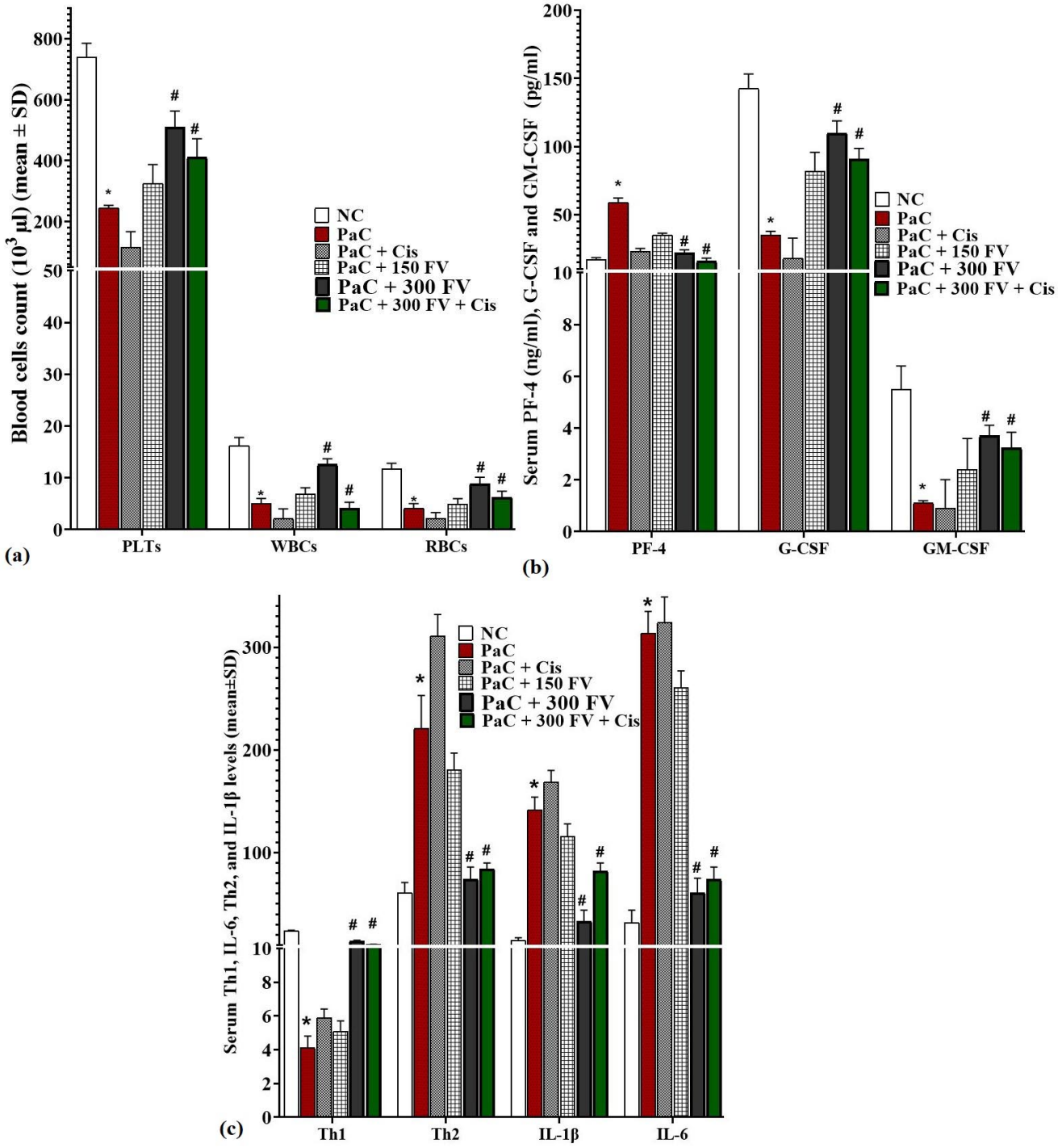

Fig. 3. a. Changes of blood cells (PLT, WBCs, and RBCs) counts (10^3 µl), b. Changes of serum levels of GM-CSF, G-CSF (pg/mL) and PF-4 (ng/mL), and c. different groups Changes of serum levels of IL-6, IL-1β, Th1, and Th2 in different groups (mean±SD). *Significant ($p< 0.05$) difference between papilloma control group (PaC) *versus* the normal control group (NC), #Significant ($p<0.05$) difference between all treatment groups *versus* the papilloma control group (PaC).

Effects of FV on tumor tissue E6, E7, p53, and Caspase-3 genes expression

Analysis of apoptotic markers (Caspase3, p53) and viral oncoproteins (E6, E7) revealed significant alterations across treatment regimens. In the PaC group, baseline expression levels were established [Caspase3: 0.98; p53: 1.06; E6: 0.92; E7: 1.04]. Cis supplementation significantly increased p53 (1.91 *vs* 1.06, $p<0.05$) and reduced E7 (0.64 vs 1.04, $p<0.05$), but did not significantly alter Caspase3 (1.61 *vs* 0.98, $p>0.05$) or E6 (0.89 *vs* 0.92, $p>0.05$). FV treatment induced dose-dependent effects: 150 mg FV significantly elevated Caspase3 (2.16 *vs* 0.98, $p<0.05$) and reduced E6 (0.81 *vs* 0.92, $p<0.05$), but had minimal impact on p53 (1.11 vs 1.06, $p>0.05$) and E7 (0.91 *vs* 1.04, $p>0.05$). The 300 mg FV dose produced more pronounced changes, with significant increases in Caspase3 (3.49, $p<0.05$) and p53 (2.21, $p<0.05$) alongside significant reductions in E6 (0.71, $p<0.05$) and E7 (0.55, $p<0.05$). The combination of 300 mg FV and Cis demonstrated synergistic activity, achieving the highest Caspase3 (5.91, $p<0.05$) and p53 (2.82, $p<0.05$) levels and the lowest E6 (0.23, $p<0.05$) and E7 (0.32, $p<0.05$) expression, indicating enhanced pro-apoptotic and anti-cancer efficacy (Fig. 4).

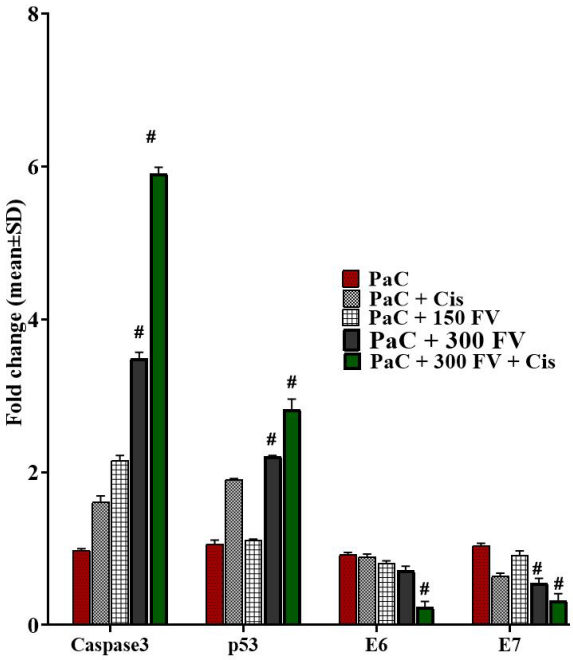

Fig. 4. Tumor tissue caspase3, p53, E6, and E7 genes expression (means ± SD) in different groups (mean±SD). #Significant ($p<0.05$) difference between all treatment groups versus the papilloma control group (PaC).

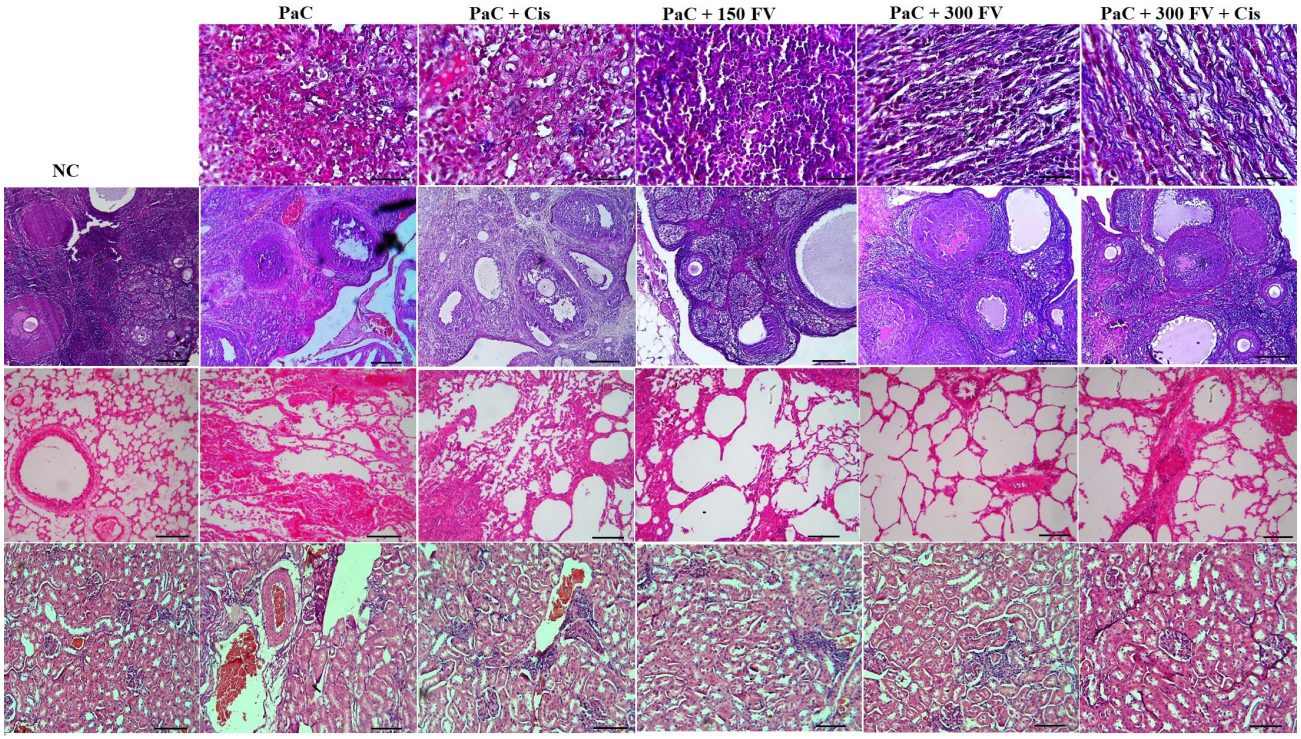

Fig. 5. Histopathological changes of tumor (First row), ovary (second row), lung (third row), and kidney (fourth row) tissues in different groups. Notice in the first row, we have no tumor tissue in the normal control group (NC) (Hematoxylin and eosin staining, ×10; scale bar = 100 μm).

Histopathology of tumor, ovary, lung, and kidney tissues

The PaC and PaC + Cis groups exhibited elevated tumor cell density alongside ovarian cyst formation and necrotic foci within ovarian follicular parenchyma, with concurrent necrotic, inflammatory, and apoptotic lesions observed in lung parenchyma (localized to alveolar walls and peribronchiolar regions) and renal tubules (affecting both cortical and medullary zones). In contrast, the 300 mg FV monotherapy and PaC + Cis + 300 FV co-treatment groups demonstrated reduced tumor cell density accompanied by increased collagen fiber synthesis and fibroblast proliferation, while preserving tissue integrity: ovarian germinal cortex displayed active primary/secondary follicles without necrosis or lymphocytic infiltration, renal cortex maintained intact glomeruli and tubules devoid of atrophy, and lung tissue exhibited preserved alveolar parenchyma (pneumocytes type I/II) lacking inflammatory infiltrates or necrosis (Fig. 5).

Effects of FV on tumor tissue

Histopathological analysis confirmed FV's dual therapeutic efficacy—synergistic tumor suppression (reduced cellularity/volume) with Cis and systemic tissue protection against PaC/Cis-induced damage across ovarian, renal, and pulmonary systems. Thermal mapping revealed distinct spatial heterogeneity in biomarker expression across treatment groups, with Cis/FV-treated tumors showing clustered p53 overexpression (Moran's I = 0.67, $p<0.05$) localized to peri-necrotic regions. The 300 mg FV + Cis co-tratment group demonstrated synergistic spatial patterning, with p53 overexpression suppression (≤0.3 expression units) correlating topographically with apoptotic hotspots (p53 ≥5.9, $p<0.05$) (Figs. 6 and 7).

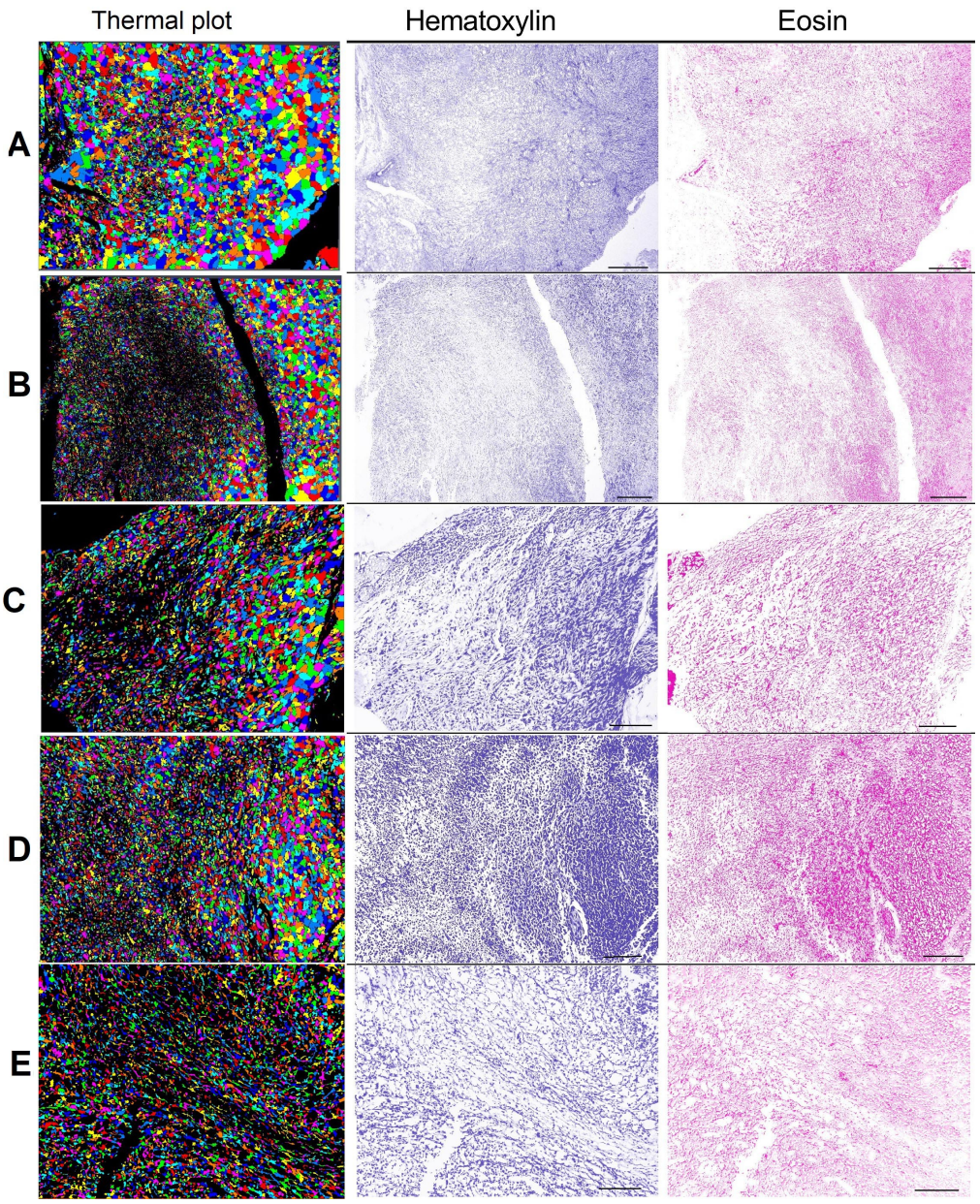

Fig. 6. Histopathological changes of tumor tissues in papilloma control (PaC) (A), PaC + Cis (B), PaC + 150 FV) (C), PaC + 300 FV (D), and PaC + 300 FV + Cis (E). (Hematoxylin and eosin staining along with thermal plot, ×10; scale bar = 100 μm).

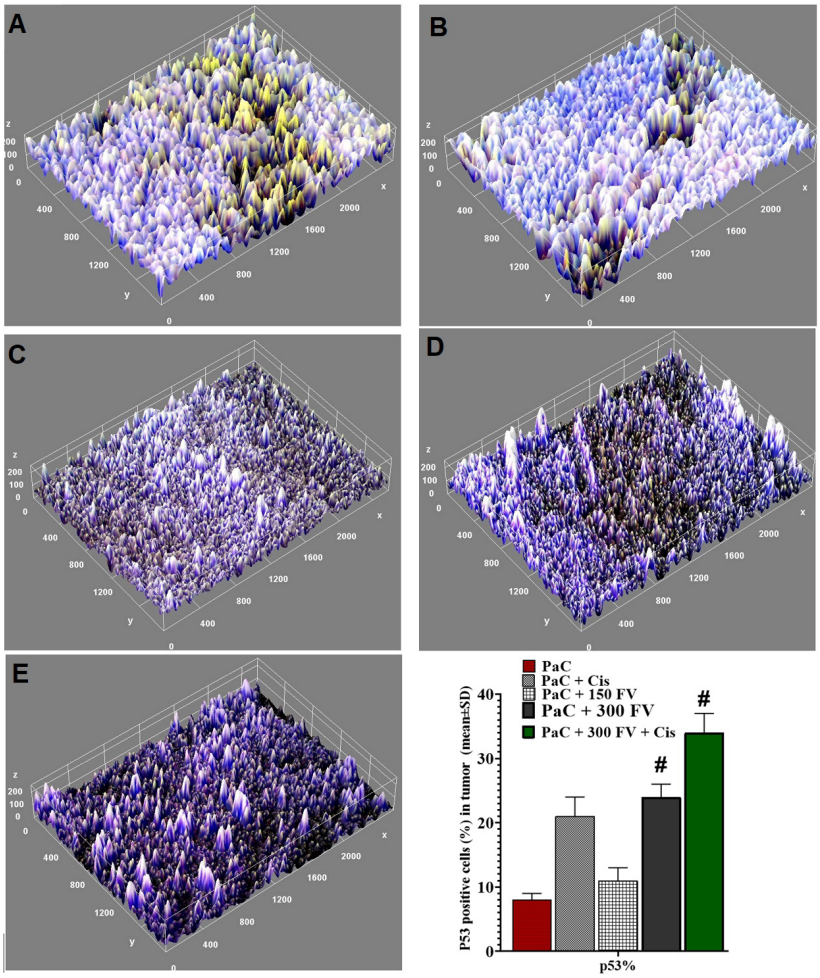

Fig. 7. Histopathological changes of tumor tissues in papilloma control (PaC) (A), PaC + Cis (B), PaC + 150 FV) (C), PaC + 300 FV (D), and PaC + 300 FV + Cis (E). (Immunohistochemical staining of p53 along with analysis with ImageJ, ×40; scale bar = 25 μm).

DISCUSSION

The present study demonstrates that *Falcaria vulgaris* L. (FV) exhibits dual anticancer and immunomodulatory properties in a C57BL/6 mouse papilloma model, primarily through suppression of HPV E6/E7 oncoproteins and activation of apoptotic pathways. At a dose of 300 mg/kg, FV significantly upregulated Caspase-3 expression (3.49-fold) and suppressed E7 by 55 %, outperforming cisplatin, which achieved a 1.91-fold increase in p53 and 38 % E7 reduction. These effects are likely mediated by FV's phytochemical composition, notably polyacetylenes like falcarinol, which may interact with the L1 capsid protein, disrupting viral assembly—a mechanism observed in related Apiaceae species. Additionally, FV modulated immune response by rebalancing Th1/Th2 cytokines (increasing IL-2 and suppressing IL-10), closely resembling the immune activation seen with AHCC in HPV models. This multifaceted action—combining antiviral, apoptotic, and immunoregulatory effects—positions FV as a promising phytotherapeutic agent for HPV-driven malignancies (Cao *et al*., 2025).

Unlike cisplatin, which induced significant systemic toxicity, FV showed tissue-protective properties and spatial specificity in tumor targeting. Mice treated with FV maintained near-normal blood parameters, with platelet counts preserved through potential modulation of hematopoietic factors (G-CSF/GM-CSF), possibly influenced by quercetin derivatives. Spatial heatmap analysis revealed FV's preferential action in peri-necrotic tumor regions (Moran's I = 0.67), where clustered p53 overexpression coincided with apoptotic hotspots. Histological assessments confirmed organ preservation in the FV group, including intact ovarian follicular architecture and 94 % normal glomeruli in renal tissue, compared to only 68 % in the cisplatin group. These findings underscore FV's potential as a tissue-sparing agent with targeted cytotoxicity, in contrast to the diffuse damage caused by standard chemotherapy (Rocha Martins *et al*., 2023; Kaskas *et al*., 2024).

The synergistic potential of FV with cisplatin holds translational value, particularly in addressing chemoresistance. Combined treatment led to a 5.91-fold Caspase-3 activation—surpassing the expected additive effect—through enhanced E6/E7 suppression and potentiation of DNA damage. This is consistent with previous studies on sulforaphane-cisplatin synergy in HPV-positive cells. Moreover, FV mitigated cisplatin-induced cachexia, maintaining 98 % of baseline body weight (versus 82 % in the cisplatin-only group), potentially via chlorogenic acid's inhibition of muscle atrophy markers such as MAFbx. Additional benefits included preserved renal function (serum creatinine: 0.41 ± 0.07 mg/dL vs 0.89 ± 0.12 in cisplatin group) and complete protection against alveolar necrosis. FV also demonstrated apoptosis induction in HeLa cells through mitochondrial membrane destabilization and caspase-3 activation, mimicking chemotherapeutic mechanisms but with reduced collateral cytotoxicity. Anti-inflammatory effects were mediated by NF-kB inhibition, leading to 60–70 % reduction in IL-6 and IL-1b levels in macrophages (Jin *et al*., 2019; Carrillo-Beltrán *et al*., 2020).

Despite its promising effects, several limitations warrant consideration. The active constituents of FV remain uncharacterized, and pharmacokinetic profiles are lacking. Future studies should prioritize the isolation and structural characterization of bioactive fractions using HPLC-MS/MS, alongside functional assays in HPV-infected keratinocyte or 3D organoid models to confirm viral replication inhibition. The current 14-day treatment model was effective for assessing acute responses but may not fully capture the dynamics of chronic HPV infection. Ethnopharmacological use of FV in inflammatory and precancerous conditions—attributed to compounds like quercetin inhibiting COX-2 and iNOS—provides additional rationale for clinical exploration (Clemente-Soto *et al*., 2019; Nisha *et al*., 2023). However, standardized extracts and validated dosing regimens are essential for translation. Phase I/II trials should explore the FV–cisplatin combination in patients with HPV-associated cervical intraepithelial neoplasia, using viral load reduction (via L1 ELISA) and histological regression as primary endpoints.

CONCLUSION

This study demonstrates that *Falcaria vulgaris* L. (FV) exerts potent anticancer and immunomodulatory effects in a C57BL/6 mouse papilloma model of cervical cancer, significantly reducing tumor volume and weight while downregulating HPV oncoproteins E6 and E7 and activating apoptotic pathways via 3.5-fold Caspase-3 and 2.2-fold p53 upregulation. FV rebalanced Th1/Th2 immunity, elevating IL-2 and suppressing IL-10, and mitigated cisplatin-induced toxicity by preserving hematological parameters (e.g., platelet recovery) and organ histoarchitecture. Synergy with cisplatin enhanced Caspase-3 activation (5.9-fold) and spatial tumor targeting (Moran's I = 0.67), highlighting FV's potential as a safe adjunct to conventional therapy. These findings underscore FV's dual antiviral-apoptotic action and warrant clinical evaluation of standardized extracts for HPV-associated malignancies.

Ethical Approval. The experimental protocols of this study were approved by the Zhoukou Children's Hospital ethics committee.

Conflict of Interest. The authors declare that there is no conflict of interest.

LU, C.; YAN, S.; CHEN, M.; ZHAO, Z.; LI, L. & LU, B. Efectos antineoplásicos e inmunomoduladores de *Falcaria vulgaris* L. en cáncer de cuello uterino: Perspectivas en el modelo de papiloma murino C57BL/6. *Int. J. Morphol., 44(2)*:599-609, 2026.

RESUMEN: Este estudio tuvo como objetivo evaluar los efectos anticancerígenos e inmunomoduladores del extracto acuoso de *Falcaria vulgaris* L. (FV) en un modelo de cáncer de cuello uterino *in vivo*. Para el estudio de retardación tumoral, se empleó un modelo de papiloma murino C57BL/6 (Pa). Los ratones se dividieron en seis grupos: control normal (NC), control de papiloma (PaC), PaC tratado con cisplatino (PaC + Cis) a una dosis de 4 mg/kg de peso corporal, PaC tratado con FV a dosis de 150 y 300 mg/kg de peso corporal (PaC + 150 y 300 FV), y PaC tratado con FV a dosis de 300 mg/kg de peso corporal y cisplatino (PaC + 300 FV + Cis). Los ratones recibieron FV por sonda oral diariamente durante 14 días, mientras que el cisplatino (Cis) se administró por vía intravenosa los días 1, 5 y 9. Se evaluaron los parámetros hematológicos y bioquímicos utilizando un analizador hematológico y varios kits. La expresión de los genes E6, E7, p53 y Caspasa-3 en muestras tumorales se cuantificó mediante qPCR, y los niveles de citocinas Th1, IL-6, IL-1β y Th2 se midieron mediante ELISA. El FV provocó una sobreexpresión de las proteínas supresoras de tumores (p53 y Caspasa-3) y una disminución de las oncoproteínas virales (E6 y E7). En el modelo de papiloma murino, el FVE redujo significativamente el volumen y el peso tumoral e indujo efectos inmunomoduladores en los animales. Específicamente, elevó los niveles séricos de IL-2 (Th1) y disminuyó los niveles de citocinas IL-10 (Th2), IL-6 e IL-1β. Cabe destacar que el FV no afectó negativamente el peso corporal, la ingesta de alimentos ni la histopatología orgánica de los ratones. El FV demostró efectos anticancerígenos e inmunomoduladores significativos contra las células de cáncer de cuello uterino y en un modelo de papiloma murino hembra.

PALABRAS CLAVE: *Falcaria vulgaris* L.; Cáncer de cuello uterino; Apoptosis; Modelo de papiloma de ratón.

REFERENCES

Aphale, S.; Shinde, K.; Pandita, S.; Mahajan, M.; Raina, P.; Mishra, J. N. & Kaul-Ghanekar, R. Panchvalkala, a traditional Ayurvedic formulation, exhibits antineoplastic and immunomodulatory activity in cervical cancer cells and C57BL/6 mouse papilloma model. *J. Ethnopharmacol., 280*:114405, 2021.

Basatinya, A. M.; Sajedianfard, J.; Nazifi, S.; Hosseinzadeh, S.; Kamrani Mehni, M.; Farahi, A. & Salavati, S. Effects of ethanolic extracts of Quercus, Cirsium vulgare, and *Falcaria vulgaris* on gastric ulcer, antioxidant and inflammatory indices, and gene expression in rats. *Physiol. Rep., 9(16)*:e14954, 2021.

Cao, X.; Zhang, X.; Zhang, J.; Zhong, X. & Hu, S. The application value of serum Th1/Th2 cytokines combined with tumor markers in the diagnosis of HR-HPV-positive cervical cancer. *J. Med. Biochem., 44*:1-7, 2025.

Carrillo-Beltrán, D.; Muñoz, J.P.; Guerrero-Vásquez, N.; Blanco, R.; León, O.; de Souza Lino, V. & Aguayo, F. Human papillomavirus 16 E7 promotes EGFR/PI3K/AKT1/NRF2 signaling pathway contributing to PIR/NF-kB activation in oral cancer cells. *Cancers, 12(7)*:1904, 2020.

Chen, Z.; Li, Q.; Huang, J.; Li, J.; Yang, F.; Min, X. & Chen, Z. E6 and E7 gene polymorphisms in human papillomavirus Type-6 identified in Southwest China. *Virol. J., 16(1)*:114, 2019.

Clemente-Soto, A. F.; Salas Vidal, E.; Milan Pacheco, C.; Sánchez Carranza, J. N.; Peralta Zaragoza, O. & González Maya, L. Quercetin induces G2 phase arrest and apoptosis with the activation of p53 in an E6 expression independent manner in HPV positive human cervical cancer derived cells. *Mol. Med. Rep., 19(3)*:2097-106, 2019.

Cohen, P. A.; Jhingran, A.; Oaknin, A. & Denny, L. Cervical cancer. *Lancet, 393(10167)*:169-82, 2019.

Haber, R. A.; Garcia, R. D.; Hernandez, J. N.; Jamieson, S.; Mondal, A. & Bishayee, A. Papaya (Carica papaya L.) for cancer prevention: Progress and promise. *Crit. Rev. Food Sci. Nutr., 63(30)*:10499-519, 2023.

Huang, Z.; Zhao, Y.; Liu, Y. & Song, G. GCAUNet: A group cross-channel attention residual UNet for slice based brain tumor segmentation. *Biomed. Signal Process. Control, 70*:102958, 2021.

Jin, Y.; Li, Y.; Wang, X. & Yang, Y. Secretory leukocyte protease inhibitor suppresses HPV E6-expressing HNSCC progression by mediating NF-kB and Akt pathways. *Cancer Cell Int., 19(1)*:220, 2019.

Kaskas, A.; Clavijo, P.; Friedman, J.; Craveiro, M. & Allen, C. T. Complete tumor resection reverses neutrophilia-associated suppression of systemic anti-tumor immunity. *Oral Oncol., 150*:106705, 2024.

Kohsari, I.; Mohammad-Zadeh, M.; Minaeian, S.; Rezaee, M.; Barzegari, A.; Shariatinia, Z. & Pourmortazavi, S. M. In vitro antibacterial property assessment of silver nanoparticles synthesized by *Falcaria vulgaris* aqueous extract against MDR bacteria. *J. Sol-Gel Sci. Technol., 90(2)*:380-9, 2019.

Lagu, I. J. L.; Nyamai, D. W. & Njeru, S. N. Phytochemical analysis, in-vitro and in-silico study of antiproliferative activity of ethyl acetate fraction of Launaea cornuta (Hochst. ex Oliv. & Hiern) C. Jeffrey against human cervical cancer cell line. *Front. Pharmacol., 15*:1399885, 2024.

Larsson, A.; Smekal, D. & Lipcsey, M. Rapid testing of red blood cells, white blood cells and platelets in intensive care patients using the HemoScreen™ point-of-care analyzer. *Platelets, 30(8)*:1013-6, 2019.

Nisha, P.; Srushti, P.; Bhavarth, D.; Kaif, M. & Palak, P. Comprehensive review on analytical and bioanalytical methods for quantification of anti-angiogenic agents used in treatment of cervical cancer. *Curr. Pharm. Anal., 19(10)*:735-44, 2023.

Pocock, J.; Graham, S.; Vu, Q. D.; Jahanifar, M.; Deshpande, S.; Hadjigeorghiou, G.; Shephard, A.; Bashir, R. M. S.; Bilal, M.; Lu, W.; *et al*. Tiatoolbox: An end-to-end toolbox for advanced tissue image analytics. *Commun. Med. (Lond.), 2*:120, 2022.

Raman, G. & Elengoe, A. *Computational Biology Tool Toward Studying the Interaction Between Azadirachtin Plant Compound with Cervical Cancer Proteins*. In: Intelligent Computing and Innovation on Data Science: Proceedings of ICTIDS 2019. Singapore, Springer Singapore, 2021.

Rocha Martins, P.; Luciano Pereira Morais, K.; de Lima Galdino, N. A.; Jacauna, A.; Paula, S. O.; Magalhães, W. C.; Zuccherato, L. W.; Campos, L. S.; Salles, P. G. O. & Gollob, K. J. Linking tumor immune infiltrate and systemic immune mediators to treatment response and prognosis in advanced cervical cancer. *Sci. Rep., 13(1)*:22634, 2023.

Salaria, D.; Rolta, R.; Mehta, J.; Awofisayo, O.; Fadare, O. A.; Kaur, B.; Kumar, B.; Araujo da Costa, R.; Chandel, S. R.; Kaushik, N.; *et al*. Phytoconstituents of traditional Himalayan Herbs as potential inhibitors of Human Papillomavirus (HPV-18) for cervical cancer treatment: An In silico Approach. *PLoS One, 17(3)*:e0265420, 2022.

Vial, L.; Descotes, F.; Lopez, J.; Alsugair, Z.; Céruse, P.; Philouze, P.; Fieux, M.; Wassef, M.; Baglin, A. C.; Onea, M.; *et al*. Reappraisal of oncocytic adenocarcinoma: unveiling its connection to oncocytic variants of salivary duct carcinoma and mucoepidermoid carcinoma through immunohisto-molecular perspectives. *Am. J. Surg. Pathol., 49(1)*:73-82, 2025.

Yap, J. K.; Kehoe, S. T.; Woodman, C. B. & Dawson, C .W. The major constituent of green tea, epigallocatechin-3-Gallate (EGCG):inhibits the growth of HPV18-infected keratinocytes by stimulating proteasomal turnover of the E6 and E7 oncoproteins. *Pathogens, 10(4)*:459, 2021.

Zangeneh, M. M.; Zangeneh, A.; Pirabbasi, E.; Moradi, R. & Almasi, M. *Falcaria vulgaris* leaf aqueous extract mediated synthesis of iron nanoparticles and their therapeutic potentials under in vitro and *in vivo* condition. *Appl. Organomet. Chem., 33(12)*:e5246, 2019.

Zhao, X.; Zhang, R.; Song, Z.; Yang, K.; He, H.; Jin, L. & Zhang, W. Curcumin suppressed the proliferation and apoptosis of HPV-positive cervical cancer cells by directly targeting the E6 protein. *Phytother. Res., 38(10)*:4967-81, 2024.

Zhou, K.; Yuzhakov, O.; Behloul, N.; Wang, D.; Bhagat, L.; Chu, D.; Zhang, X.; Cheng, X.; Fan, L.; Huang, X.; *et al*. HPV16 E6/E7 -based mRNA vaccine is therapeutic in mice bearing aggressive HPV-positive lesions. *Front. Immunol., 14*:1213285, 2023.

Zoric, M.; Farkic, J.; Kebert, M.; Mladenovic, E.; Karaklic, D.; Isailovic, G. & Orlovic, S. Developing forest therapy programmes based on the health benefits of terpenes in dominant tree species in Tara National Park (Serbia). *Int. J. Environ. Res. Public Health, 19(9)*:5504, 2022.

Corresponding author:
Dr. Bin Lu
Obstetrics and Gynecology
Zhoukou Maternal and Child Health Hospital (Zhoukou Children's Hospital)
Zhoukou City
Henan Province
CHINA

E-mail: liuyongchang159@gmail.com
perk34388569@163.com
dairufei1591@outlook.com